locality of neural field models. Even though the calculation uses information from only the leading edge of a wave it gives wave speed predictions in very good agreement with those from direct numerical simulations. In section IV we consider a Heaviside firing rate function and focus on time-independent spatially varying solutions and show how to determine existence and stability of pinned front solutions. A fully nonlinear analysis of traveling fronts is developed in section V based on tracking the evolution of level set contours of the neural activity. For a Heaviside firing rate this interface dynamics simplifies considerably and the dynamics for a traveling front is determined by a single scalar nonlinear ordinary differential equation (ODE). For weak modulation this ODE can be analyzed using standard perturbation arguments and the wave speed of a pulsating front is easily calculated. Once again the theory is in excellent agreement with numerical simulations and, in contrast to results obtained using homogenization theory, can describe wave behavior even when the period modulation of the spatial kernel is not rapid. Finally in section VI we summarize and discuss possible extensions of this work.

II. THE MODEL

Many current coarse grained models of neural tissue trace their origins back to seminal work in the 1970s by Wilson and Cowan [13, 14] and Amari [15, 16]. In one spatial dimension the simplest single population model that describes the evolution of neural activity $u = u(x, t)$, with $x \in R$ and $t \in R^+$ is

$$u_t = -u + \psi, \qquad \psi(x, t) = \int_{-\infty}^{\infty} dy\, W(x, y) f\left(u(y, t)\right). \quad (1)$$

The function f represents the firing rate of the tissue and is often chosen to have a sigmoidal form. The weight kernel $W(x, y)$ represents anatomical connectivity between points x and y in the tissue and the presence of this function means that the model has a non-local structure. For a more comprehensive discussion of such models, their generalization and their use in neuroscience we refer the reader to [17]. In this paper we mostly focus on a very specific form of heterogeneity, namely one where the connectivity has the following product structure:

$$W(x, y) = W(|x - y|) J(y), \qquad J(y) = J(y + \ell), \quad (2)$$

where J is some ℓ-periodic function. The use of periodically modulated translationally-invariant kernels of this form is particularly relevant to modeling primary visual cortex, which is known to have a periodic micro-structure on the millimeter scale, reviewed in some detail in the paper by Bressloff [6]. For later convenience we shall use a Fourier representation for the real periodic function J and write

$$J(x) = \sum_n J_n e^{2\pi inx/\ell}, \qquad J_{-n} = J_n^\dagger, \quad (3)$$
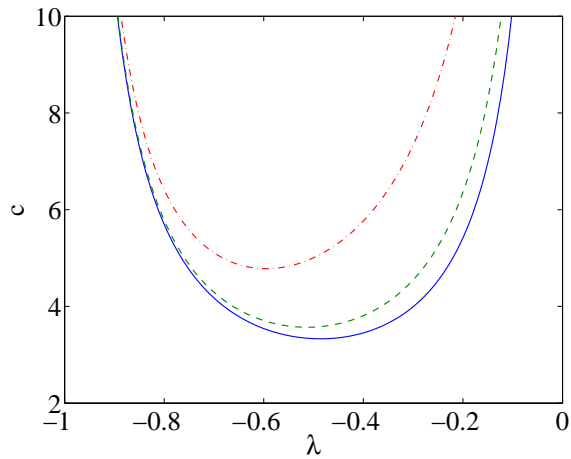
FIG. 2. (Color online). A plot of the wave speed estimate c as a function of λ defined by $\det A(c, \lambda) = 0$ with $N = 20$ for three values of ϵ. $\epsilon = 1.5$ (red, dash-dotted), $\epsilon = 0.5$ (green, dashed) and $\epsilon = 0$ (blue, solid). Other parameters are $\gamma = 2$, $J_0 = 1, \sigma = 2\pi$.

and the fixed point at $u = 0$ is unstable for small   when $-1 + \ J_0 > 0$ (as can be seen by considering spatially coherent perturbations of the form $u(x, t) =$ $\exp(\ t)$ in equation (6) and demanding that Re < 0).

B.   Numerical Results

A plot of c as a function of , defined by the relation $\det A(c, \ ) = 0$, is shown in Fig. 2 for various values of . Here it can be seen that $c = c(\ )$ has a well defined minimum, c^*

where

$$L(\xi) = \int_0^\infty dy\, W(y) J'(\xi - y) = \frac{dq(\xi)}{d\xi}. \quad (28)$$

Hence, solutions with $dq(\xi)/d\xi < 0$ are stable and those with $dq(\xi)/d\xi > 0$ are unstable. For the example of Fig. 5 we see from Fig. 6 that of the two possible solutions it is the one with largest Δ that is stable.

V. INTERFACE DYNAMICS

Motivated by the form of the pulsating front in Fig. 1 we seek to describe the properties of this solution solely in terms of the behavior at the front edge which separates high activity from low. If the front is not pulsating (which is the case in the absence of period modulation of the connectivity) then in a traveling wave frame (of the same speed as the wave) the rising edge of the front may be identified with a single (traveling wave) co-ordinate. For a pulsating front this point is no longer stationary in time and instead oscillates. We now show how to derive the dynamics for this interface between high and low activity states.

In a co-moving frame the model (1) takes the form $u = u(\xi, t)$ where $\xi = x - c_0 t$ for some fixed c_0 and

$$-c_0 u_\xi + u_t = -u + \psi, \quad (29)$$

where

$$\psi(\xi, t) = \int_{-\infty}^{\infty} dy\, W(\xi + c_0 t, y) f\left(u(y - c_0 t, t)\right). \quad (30)$$

We define a moving interface (level set) according to

$$u(\xi_0(t), t) = h, \quad (31)$$

for some constant h. Here we are assuming that there is only one point on the interface (though in principle we could consider a set of points). Differentiation of (31) gives an exact expression for the velocity of the interface in the form

$$\dot{\xi}_0 = -\left.\frac{u_t}{u_\xi}\right|_{\xi = \xi_0(t)}. \quad (32)$$

Focusing now on the case of a Heaviside firing rate with $f(u) = f_2(u)$ means that for a pulsating front solution with $u > h$ for $\xi < \xi_0$ (30) takes the simple form

$$\psi(\xi, t) = \int_{-\infty}^{\xi_0 + c_0 t} dy\, W(\xi + c_0 t, y). \quad (33)$$

A. Perturbation analysis

Consider a perturbation around the unmodulated case and write $W(x, y) = W(|x - y|)[1 + \epsilon K(y)]$ ($K(y) =$ $K(y + \Delta)$) for some small parameter ϵ. For $\epsilon = 0$ there is a traveling front $q(\xi)$ given by the solution of

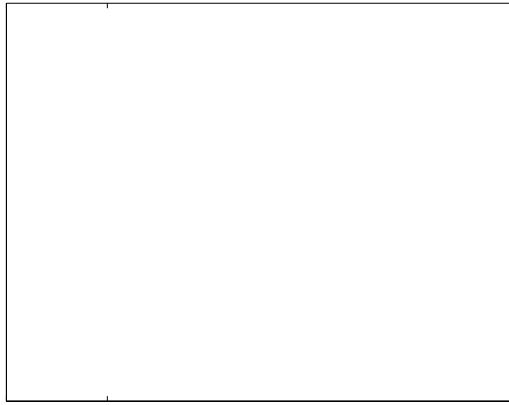$$-c_0 \frac{dq}{d\xi} = -q + \psi, \qquad \psi(\xi) = \int_\xi^\infty dy\, W(|y|), \quad (34)$$

where the speed c_0 is determined by $q(0) = h$. For small ϵ we assume that the slope of the traveling front varies sufficiently slowly so that we may make the convenient approximation $u_\xi|_{\xi = \xi_0(t)} = q_\xi|_{\xi = 0}$. In this case we have, using equations (29) and (34), that

$$u_t|_{\xi = \xi_0(t)} = \int_{-\infty}^{\xi_0 + c_0 t} dy\, W(\xi_0 + c_0 t, y) - \int_0^\infty dy\, W(|y|), \quad (35)$$

$$u_\xi|_{\xi = \xi_0(t)} = \frac{1}{c_0}\left[h - \int_0^\infty dy\, W(|y|)\right]. \quad (36)$$

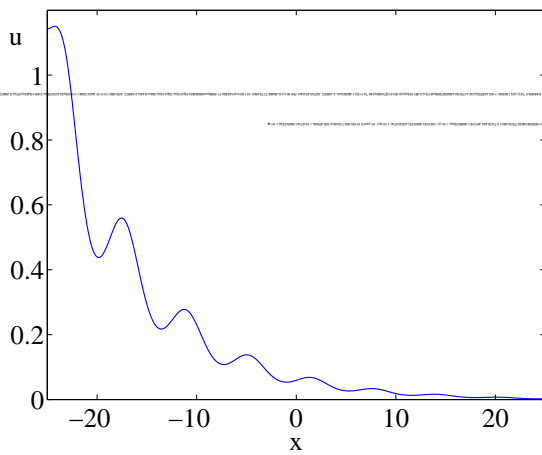Substitution of equations (35) and (36) into equation (32) gives

$$\dot{\xi}_0 = c_0\, \frac{\int_0^\infty dy\, W(|y|) K(\ldots)}{\int_0^\infty dy\, W(|y|) K(\ldots)}.$$

0

FIG. 11. (Color online). A stationary solution of (1)-(2) for $f = f_1$. Parameters are $\gamma = 0.95, J_0 = 1, \sigma = 2\pi, \epsilon = 0.3$.

point at which $q(y) = h$. Comparing Figs. 4 and 7 it is interesting to note that the speed of a front increases as is increased when $f = f_1$ and decreases as is increased when $f = f_2$. This demonstrates that the qualitative behavior of a model such as (1)-(2) can depend on the exact form of the nonlinear function f. The only reasonable way to compare results obtained for $f = f_1$ and $f = f_2$ would be to take in f_1 and h 0 in f_2. However, the result would be $f(u) = H(u)$, the unshifted Heaviside, for which the speed of a front in the

unmodulated case is infinite $[c_0 = (1 - 2h)/(2h)]$. Thus, a meaningful comparison is not really possible and our methods and results ca5.884847(t)2.55846914lt6l 1192.476956.5

100, 371 (2009).

[29] G. J. Lord and V. Thümmler, arXiv:1006.0428v1 (2010).